Geomechanics and Engineering, *Vol. 27, No. 4 (2021) 361-374*
https://doi.org/10.12989/gae.2021.27.4.361

Physics-based reduced order model for computational geomechanics

Hongbo Zhao*[1] and Bingrui Chen[2a]

[1]*School of Civil and architectural Engineering, Shandong University of Technology, Zibo, 255000, People's Republic of China*
[2]*Wuhan Institute of Rock and Soil mechanics, Chinese Academy of Sciences, Wuhan, 430071, People's Republic of China*

(Received May 17, 2020, Revised October 20, 2021, Accepted October 21, 2021)

Abstract. Numerical models are an essential tool in stability analysis, design, and construction for geotechnical engineering. Yet, numerical modeling is too time-consuming in practical engineering. In this study, a physics-based reduced order model (ROM) was developed to approximate the displacement and stress field of geotechnical structure by combining Latin hypercube sampling (LHS), a numerical method and proper orthogonal decomposition (POD). The set of design variables were constructed using LHS. A numerical model was used to generate the snapshots based on the design variables. POD was used to compute the eigenvalues and eigenvectors of a spatial Gram matrix, which was constructed based on snapshots. The first K eigenfunction vectors were determined based on eigenvalues and eigenvectors of the spatial Gram matrix. The interpolation matrix of elements was computed using a radial basin function (RBF), and then the vector of an element was determined by solving the penalized linear systems. To determine the new design variables, the coefficient of ROM was determined based on the RBF and the vector of elements, and the unknown field variables were predicted based on the ROM. The ROM was illustrated and verified for a circular tunnel. The results showed that the predicted displacement and stress field were in excellent agreement with both the analytical and numerical solutions. The physics-based ROM characterized well the deformation and failure mechanism of the surrounding rock mass and can be used to replace a numerical model for back analysis, optimal design, and uncertainty analysis of geotechnical engineering, thereby eliminating costly repetitive computations.

Keywords: data-driven; geomechanics; numerical model; proper orthogonal decomposition; reduced-order model

1. Introduction

Numerical modeling techniques such as the finite different method and finite element method, etc., provide very accurate predictions of the mechanical behavior of geomaterials and the stability of geotechnical engineering structures (Jing and Hudson 2002). Numerical modeling is an essential part of stability analysis, design, and construction in the profession of geotechnical engineering (Jain and Chakraborty 2018, Oh *et al*. 2019, Aksoy *et al*. 2019, Li *et al*. 2021). Yet, numerical modeling is too time-consuming in practical engineering practice because of the need for repetitive computations, such as back analysis, optimal design, and reliability analysis, etc. This shortcoming has motivated researchers to develop alternative models to replace numerical models in practical geotechnical engineering applications.

The response surface method (RSM) provides an efficient alternative model to approximate the limited state function for reliability analysis of complex engineering systems (Kathirvel and Kaliyaperumal 2017, Myers *et al*. 2009, Thakur *et al*. 2019, Zhang *et al*. 2020, Saseendran and Dodagoudar 2020). Various RSM models have been developed to approximate the response variables such as deformation, safety factors, and stress of geotechnical structures. A polynomial RSM is commonly used in reliability analysis for geotechnical engineering (Li *et al*. 2016, Hamrouni *et al*. 2018). However, approximating a complex nonlinear function using polynomial RSM is difficult in practical geotechnical engineering.

Artificial neural networks (ANN) were adopted to approximate the complex, nonlinear and implicit limited state function of the reliability analysis for engineering structures (Cardoso *et al*. 2008, Luat *et al*. 2020, Liu *et al*. 2021). ANN was widely adopted in reliability analysis to approximate the response of geomaterial (Pichler *et al*. 2003, Gomes and Awruch 2004, Lopes *et al*. 2010, Lv and Low 2011, Rafiai and Moosavi 2012, Mahdevari and Torabi 2012, Mahdevari *et al*. 2012, Mathew *et al*. 2020). In back analysis, ANN was used to approximate the relationship between geomechanical parameters and displacement of surrounding rock mass, and then determine the geomechanical parameters (You 2014).

Nevertheless, ANN has some limitations such as over-fitting, finding local minimum solutions, etc. To overcome these disadvantages, Feng *et al*. introduced a support vector machine (SVM) to construct the RSM for geotechnical engineering (Feng *et al*. 2004). SVM was used to approximate the safety factor of slope and obtain the explicit limited state function for reliability analysis of slope (Zhao 2008). SVM was also adopted to approximate displacement for determining geomaterial mechanical parameters by back analysis (Zhao and Yin 2009). To overcome the limitations of traditional SVM, a multi-output support vector machine was developed to build the RSM in

*Corresponding author, Professor
E-mail: bxhbzhao@hotmail.com
[a] Ph.D.
E-mail: brchen@whrsm.ac.cn

ISSN: 2005-307X (Print), 2092-6219 (Online)

back analysis (Zhao and Yin 2016). However, the RSM was only a universal approximator trained using a set of samples and did not reflect physical knowledge about the engineering structure (Audouze *et al*. 2009). In the alternative models just described, samples or data were used to construct a response function for approximating the actual response. Unfortunately, these models did not reflect the physical mechanism of the engineering structures.

The recent developments in data sciences provide a good way to reveal the mechanism behind data (Lecun *et al*. 2015). Data sciences have been successfully applied in the field of medicine (Veer and Bernards 2008), energy (Severson *et al*. 2019), biology (Alipanahi *et al*. 2015, Huys *et al*. 2016), and geoscience (Markus *et al*. 2019). Recently, a physics-based reduced order model (ROM) was developed that contains some knowledge about the engineering structure under consideration (Bhattacharjee and Matouš 2020). Recently, various surrogated model was developed to handle the engineering problem. A deep-learning-based surrogate model was developed and applied for predicting dynamic subsurface flow in channelized geological models (Tang *et al*. 2020). A machine learning-based data driven approach was developed to identify geology during tunnel excavation (Bai *et al*. 2021). A physics-informed deep learning framework was developed and regarded as a surrogated model to study solid mechanics (Haghighat *et al*. 2021). Zhao (2021) developed a surrogated model to improve the efficiency of the numerical analysis by combining the ROM model and machine learning (Zhao 2021). Bayesian inference was adopted to determine the geomechanical parameters and their uncertainty using a multi-output support vector machine-based surrogated model (Zhao *et al*. 2021). To improve the efficiency of back analysis, a reduced-order model was used to replace the numerical model to determine the mechanical parameters of geomaterials (Zhao *et al*. 2021). In this study, a novel computational framework of geomechanics was developed to construct the model of geomechanics by combining data-driven analyses and the physics-based ROM.

Proper orthogonal decomposition (POD) is a popular physics-based ROM that has been used in a variety of fields (Fic *et al*. 2006, Cizmas *et al*. 2008, Freno and Cizmas 2014, Luo *et al*. 2015). In this study, Latin hypercube sampling (LHS) was used to construct a set of design variables. A snapshot (sample) was generated based on numerical simulation. Then, POD was used to determine a ROM. The remainder of this paper is organized as follows. Firstly, the ROM is described in detail. Then, a circular tunnel was used to verify and illustrate the physics-based data-driven model. The detailed procedure, results and a comparison are also presented and discussed. Conclusions based on the study results are given.

2. Physics-based reduced order model

In geomechanics and geotechnical engineering, the responses such as displacement, stress, and strain field of a geotechnical structure (slope, tunnel, etc.) are functions of the geometry and size of the structure, boundary conditions, in situ stress, and mechanical parameters of geomaterial, etc. A physics-based ROM of these fields (responses) can be obtained by POD (Kenneth *et al*. 2000).

2.1 Numerical model of geotechnical engineering

A field (such as stress, strain, and displacement, etc.) of a geotechnical structure can be characterized by physical laws and governing equations, which are often represented in the form of partial differential equations (PDE) (Zienkiewicz *et al*. 2005). We consider a general nonlinear steady state PDE in R^{d}.

$$N(u(\boldsymbol{x},\boldsymbol{\theta}),\boldsymbol{\theta}) = f(u(\boldsymbol{x},\boldsymbol{\theta}),\boldsymbol{\theta}) \qquad in \quad \Omega \tag{1}$$

$$u(\boldsymbol{x},\boldsymbol{\theta}) = g(\boldsymbol{x},\boldsymbol{\theta}) \qquad on \quad \partial\Omega \tag{2}$$

In Equations (1) and (2), $\boldsymbol{x}$ represents the spatial coordinates, $\boldsymbol{\theta}$ is the vector of design variables such as mechanical parameters of geomaterial and in-situ stress, etc., u is the field variables such as stress, displacement, etc., f is the load, g is the boundary conditions, Ω is the physical space with regular boundary $\partial\Omega$, and N is the operator of the PDE. To geomechanics, the momentum balance equation is the following partial differential equation.

$$\sigma_{ij,j} + f_i = 0 \tag{3}$$

Where f_i is the body force, σ_{ij} denotes the Cauchy stress tensor. The subscript comma denotes partial derivative. To the plane problem of geomechanics, i, j equals x, y in the Cartesian coordinate system. Under the action of external forces, the deformation u and strain ε satisfy the following kinematic equation.

$$\varepsilon_{ij} = \frac{1}{2}(\mathrm{u}_{i,j} + \mathrm{u}_{j,i}) \tag{4}$$

Where u_i is the deformation (displacement), ε_{ij} is the infinitesimal strain tensor. In the elastoplastic problem of geomechanics, the strain tenson can decompose the elastic strain ε_{ij}^{e} and plastic strain ε_{ij}^{p}.

$$\varepsilon_{ij} = \varepsilon_{ij}^{e} + \varepsilon_{ij}^{p} \tag{5}$$

The stress tensor is now linearly dependent on the elastic strain tensor ε_{ij}^{e}. The plastic strain ε_{ij}^{p} .is relation to the plasticity model and meets the corresponding plasticity model.

$$\varepsilon_{ij}^{p} = \gamma \frac{\partial F}{\partial \sigma_{ij}} \tag{6}$$

Where γ is the plastic multiplier, subject to the conditions $\gamma \geq 0$. F is the yield surface and depends on the plasticity model.

$$\sigma_{ij} = \frac{E\upsilon}{(1+\upsilon)(1-2\upsilon)}\varepsilon_{kk}^{e}\delta_{ij} + \frac{E}{(1+\upsilon)}\varepsilon_{jj}^{e} \tag{7}$$

Where δ_{ij} is the Kronecker delta, E and υ is the Elastic modulus and Poisson's ratio of geomaterials, respectively.

The PDEs of geomechanics characterize well the deformation and failure mechanism of geomaterials. However, it is not easy to obtain an analytical solution for PDEs because of the complexity of geotechnical engineering applications. Thus, numerical technology is a technique for solving the above partial differential equations (Eqs.3,4,7) by discretizing these equations into linear equation groups and boundary conditions. The boundary conditions are essential to the elastic solution of solid. The finite element method (FEM) is commonly used for numerical technology. FEM has been widely used in various fields of geotechnical engineerings, such as slope stability analysis, the displacement prediction of tunnel excavation, support structure stability analysis, T-H-M-C coupling analysis, Etc. (Jing and Hudson, 2002). In this study, a physics-based ROM was developed to compute the expansion basis and its coefficient using POD. The expansion basis reduced the high-dimension numerical model to a low-dimension reduced-order model.

2.2 Physics-based reduced-order model

As stated above, the displacement and stress fields $u^h(x,\theta)$ in geomechanics can be obtained by solving the PDE using numerical technology. In this study, the ROM model was used to approximate the displacement and stress fields $u^h(x,\theta)$ in geomechanics. According to the ROM theory (Audouze *et al*. 2009), the field variables in Eqs. (1) and (2) can be presented in the following form.

$$\tilde{u}^h(x,\theta) = \sum_{k=1}^{K} \beta_k(\theta)\varphi^k(x) + \tilde{g}(x,\theta) \tag{8}$$

Where $\tilde{u}^h(x,\theta)$ is the approximated field variables using ROM model, $\varphi^k(x)$ is the eigenfunction, $\beta_k(\theta)$ is an undetermined coefficient, K is the number of eigenfunctions. K, $\varphi^k(x)$ and $\beta_k(\theta)$ can be determined using POD in this study. $\tilde{g}(x,\theta)$ is an extension of the boundary conditions in the whole domain.

$$\tilde{g}(x,\theta) = \begin{cases} g(x,\theta) & on \quad \partial\Omega \\ 0 & elsewhere \end{cases} \tag{9}$$

To obtain the ROM model, some snapshots are necessary. Firstly, LHS was used to build the set of design variables $\theta_j, j = 1,2,\dots,J$. Then a set of discrete solutions (snapshot) of PDE, $w_j = u^h(\theta_j) - \tilde{g}(\theta_j), j = 1,2,\dots,J$, was obtained using a numerical method such as finite element analysis. Let us denote by $\mathbf{M}^{\mathrm{x}}$ the spatial Gram matrix:

$$M_{ij}^{x} = (w_i \cdot w_j), i,j = 1,2,\dots,J \tag{10}$$

where $(w_i \cdot w_j)$ is the scalar product between w_i and w_j.

The positive eigenvalues λ of $\mathbf{M}^{\mathrm{x}}$ are arranged in descending order.

$$\lambda_1 \geq \lambda_2 \geq \cdots \geq \lambda_J \geq 0 \tag{11}$$

The first K eigenfunctions $\varphi^k(x), k = 1,2,..K$ associated with the first K eigenvalues provide the orthogonal principal direction of snapshots. If $r^k = (r_j^k)_{j=i,i,\dots J}$ is the k^{th} eigenvector of $\mathbf{M}^{\mathrm{x}}$, then its dual k^{th} eigenfunction $\varphi^k(x)$ is obtained using Equation (12):

$$\varphi^k(x) = \sum_{j=1}^{K} r_j^k w_j(x) \tag{12}$$

where K is the dimension of the POD basis and can be obtained using Equation (13).

$$\frac{\sum_{i=1}^{K}\lambda_i}{\sum_{i=1}^{J}\lambda_i} > k \tag{13}$$

where k is the user-specified tolerance. In this study, k was taken to be 0.99999.

For any x_i, i = 1, 2,…,I, and θ_j, j = 1, 2,…J, we can obtain Equation (8). The ROM model Equation (8) can be written in the form of Equation (14).

$$\tilde{u}^h = \varphi\beta + \tilde{g} \tag{14}$$

The unknown coefficient β can be obtained by solving the following penalized minimization problem.

$$\min_{\beta_j \in R^K} \left\| u^{h,j} - \varphi\beta_j - \tilde{g}_j \right\|^2 + \mu \left\| \beta_j \right\|^2 \tag{15}$$

for which $\beta_j$can be obtained by solving the following normal equation:

$$(\varphi^T\varphi + \mu I_K)\beta_j = \varphi^T\left(u^{h,j} - \tilde{g}_j\right), \qquad j = 1,2,\dots,J \tag{16}$$

where μ is a small regularization parameter.

To determine the field variables for unknown design variables θ and space variables x, the coefficient $\beta_k(\theta)$ is expanded using a radial basis function (RBF) as Equation (17).

$$\beta_k(\theta) = \sum_{j=1}^{J} \alpha_{jk}\psi\left(\frac{|\theta - \theta_j|}{\sigma}\right) \tag{17}$$

For any $\theta_{j'}, j' = 1,2,\dots,J$, Equation (18) can be obtained based on Equation (17):

$$\sum_{j=1}^{J} \alpha_{jk}\psi\left(\frac{|\theta_{j'} - \theta_j|}{\sigma}\right) = \beta_{kj'} \tag{18}$$

where $\beta_{kj'}$ has been obtained using Equation (17). The above equations can be written in the compact form of Equation (19),

$$A\alpha_k = \beta_k \tag{19}$$

in which the unknown coefficient α_k can be obtained by solving Equation (20).

$$\left(A^TA + \mu I_J\right)\alpha_k = A^T\beta_k, \qquad k = 1,2,\dots,K \tag{20}$$

2.3 Procedure of physics-based ROM

The physics-based ROM developed in this study is summarized in Fig.1. LHS was used to build the set of

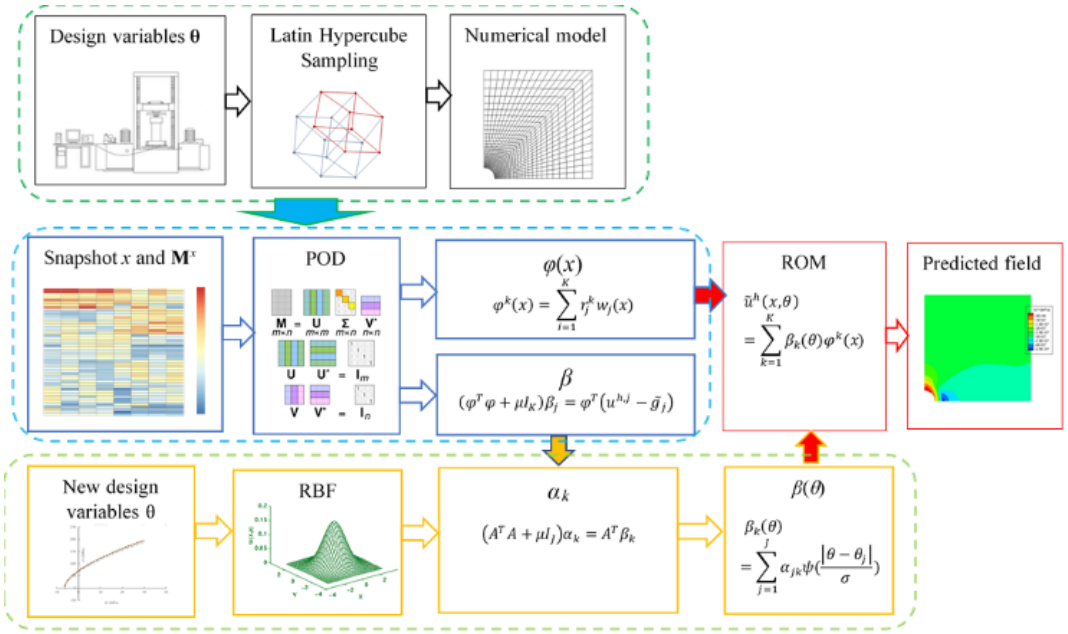

Fig. 1 The physics-based reduced-order model

design variables for the numerical model. Then the numerical model was used to generate the snapshot corresponding to each design variable in the set. Based on these snapshots, POD was used to compute the POD basis vector and its coefficient considering the physical mechanism of the engineering problem. To approximate a new design variable, RBF was used to expand the coefficient of the POD basis, and then solve the coefficients of ROM decomposition. The unknown field variables corresponding to new design variables were predicted based on the physics-based ROM.

The procedure just described involved the following steps.

Step 1: Collect the geotechnical engineering data such as in situ stress, geomaterial mechanical parameters, and boundary conditions, etc.

Step 2: Build the numerical model (FEM) based on the assembled engineering information.

Step 3: Generate the set of design variables $\boldsymbol{\theta}$ for the numerical model using LHS.

Step 4: Compute the field variables w_i (displacement or stress field) at space domain $\mathbf{X}$ using a numerical model for each design variable. Collect all the field variables and obtain the snapshots.

Step 5: Construct the spatial Gram matrix $\mathbf{M}^x$ based on the above snapshots.

Seep 6: Compute the eigenvalues $\boldsymbol{\lambda}$ and eigenvectors $\boldsymbol{r}$ based on spatial Gram matrix.

Step 7: Determine the rank number K of $\mathbf{M}^x$ and first K eigenfunction vector $\boldsymbol{\varphi}$.

Step 8: Compute the undetermined coefficient β based on the eigenfunction vector $\boldsymbol{\varphi}$ and snapshots.

Step 9: To estimate a new design variable θ, construct element ϕ based the design variables $\boldsymbol{\theta}$ that are generated by LHS using RBF.

Step 10: Compute the interpolation matrix $\mathbf{A}$ of elements ϕ.

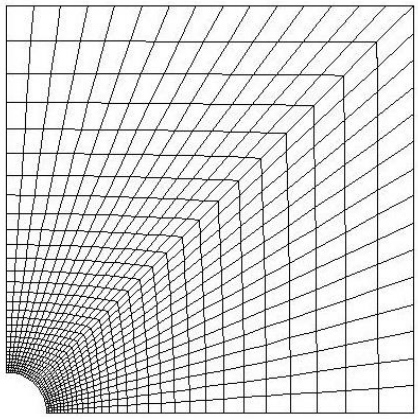

Fig. 2 Numerical model for circular tunnel

Step 11: Compute the vector of element $\boldsymbol{\alpha}$ using the penalized linear systems.

Step 12: Determine the coefficients $\beta(\theta)$ based on RBF.

Step 13: Predict the unknown field variables $\tilde{u}^h(\theta)$ based on coefficients $\beta(\theta)$ and the eigenfunction vector $\boldsymbol{\varphi}$ using ROM.

3. Numerical example

To illustrate and demonstrate the developed method, a circular tunnel subject to hydrostatic stress was studied for the Mohr-Coulomb criterion (Duncan 1993). In this study, the analytical and numerical solutions of the circular tunnel were used to illustrate and verify the validity of the ROM model. Suppose a circular tunnel is excavated in a continuous, homogeneous, isotropic, initially elastic rock mass subjected to hydrostatic far-field stress p_0 and uniform support pressure p_i. While p_i is less than the critical pressure p_{cr}, a plastic zone exists. The values of p_{cr} are obtained from

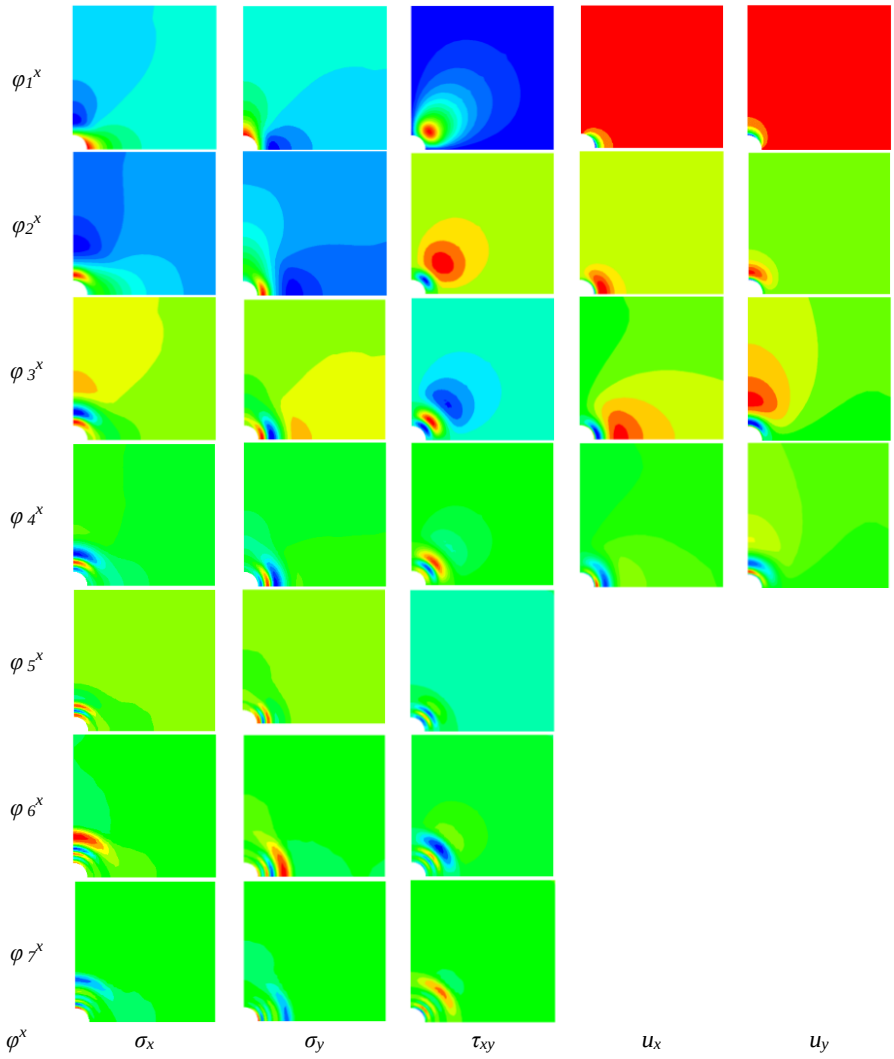

Fig. 3 The first seven and four spatial POD modes

the following equations.

$$p_{cr} = \frac{2p_0 - \sigma_c}{k+1} \tag{21}$$

where σ_c is the uniaxial compression strength, which the following equation can determine.

$$\sigma_c = \frac{c(k-1)}{\tan\varphi} \tag{22}$$

Where φ is the internal friction angle, and c is the cohesion and $k = \frac{1+\sin\varphi}{1-\sin\varphi}$.

Duncan (1993) obtained the plastic zone radius r_p and the inward displacement of tunnel wall u_{ip} based on the Mohr-Coulomb criterion.

$$\frac{r_p}{r_0} = \left[\frac{2(p_0+s)}{(k+1)(p_i+s)}\right]^{1/(k-1)} \tag{23}$$

$$\frac{u_{ip}}{r_0} = \left[\frac{1+\mu}{E}\right]\left[2(1-\mu)(p_0-p_{cr})\left(\frac{r_p}{r_0}\right)^2 - 2(1-2\mu)(p_0-p_i)\right] \tag{24}$$

where E is the elastic modulus and μ is Poisson's ratio. The values of s are obtained from the following equations:

$$s = \frac{\sigma_c}{k-1} \tag{25}$$

The physics-based ROM was applied to a circular rock tunnel to illustrate its use. The radius of the tunnel was 1 m. The surrounding rock mass is assumed to be linearly elastic and perfectly plastic. The plane strain conditions are applicable. The Mohr-Coulomb criterion and associated flow rules were adopted in the numerical model. The elastic modulus, Poisson's ratio, cohesion and friction angle of rock mechanical parameters were 6.8 GPa, 0.2, 3.45 MPa, and 30°, respectively. The isotropic in situ stress had a magnitude of -30 MPa. The FLAC3D numerical model (Itasca 2009) was adopted to build snapshots for ROM. Only a quarter of the tunnel was analyzed because of the symmetry (Fig.2). The circular tunnel was discretized into 900 elements and 1,822 nodes for numerical modeling.

The elastic modulus, Poisson's ratio, cohesion, friction angle, and in situ stress were selected as the design variables. Displacement and stress of the surrounding rock mass were the field variables. LHS was used to construct 50

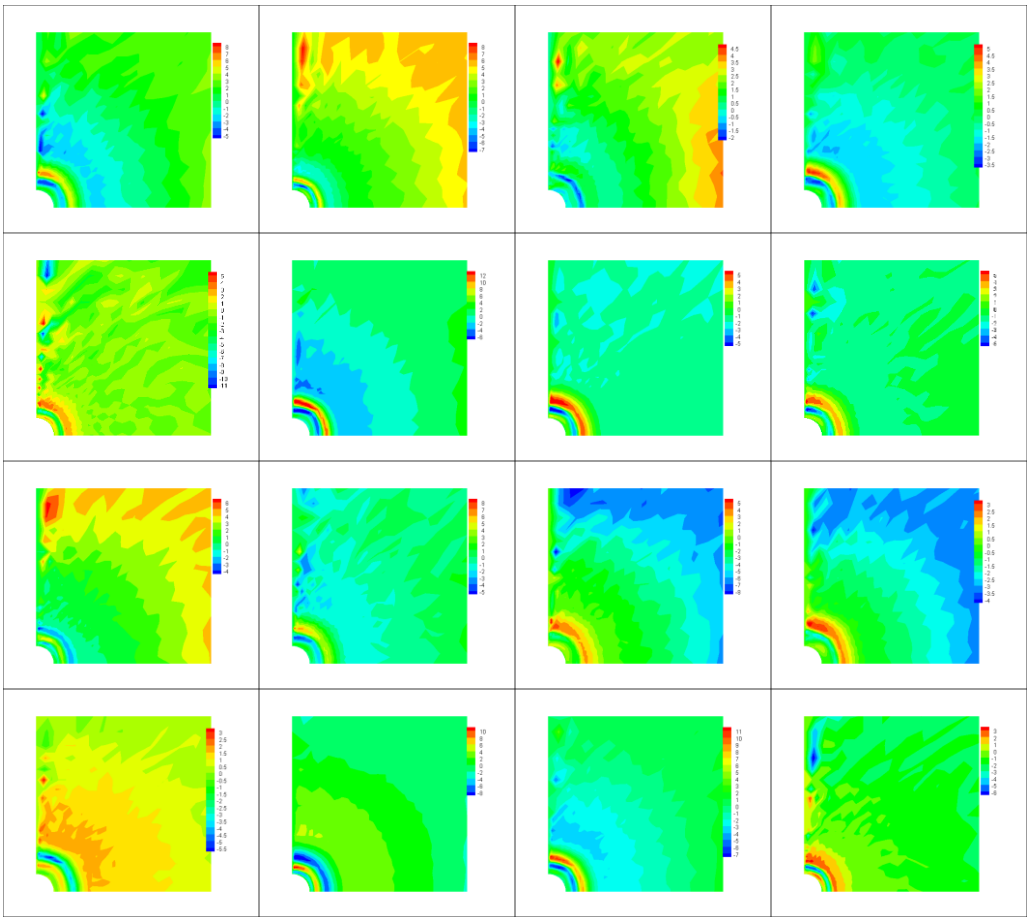

Fig. 4 The relative error of horizontal displacement for 20 snapshots

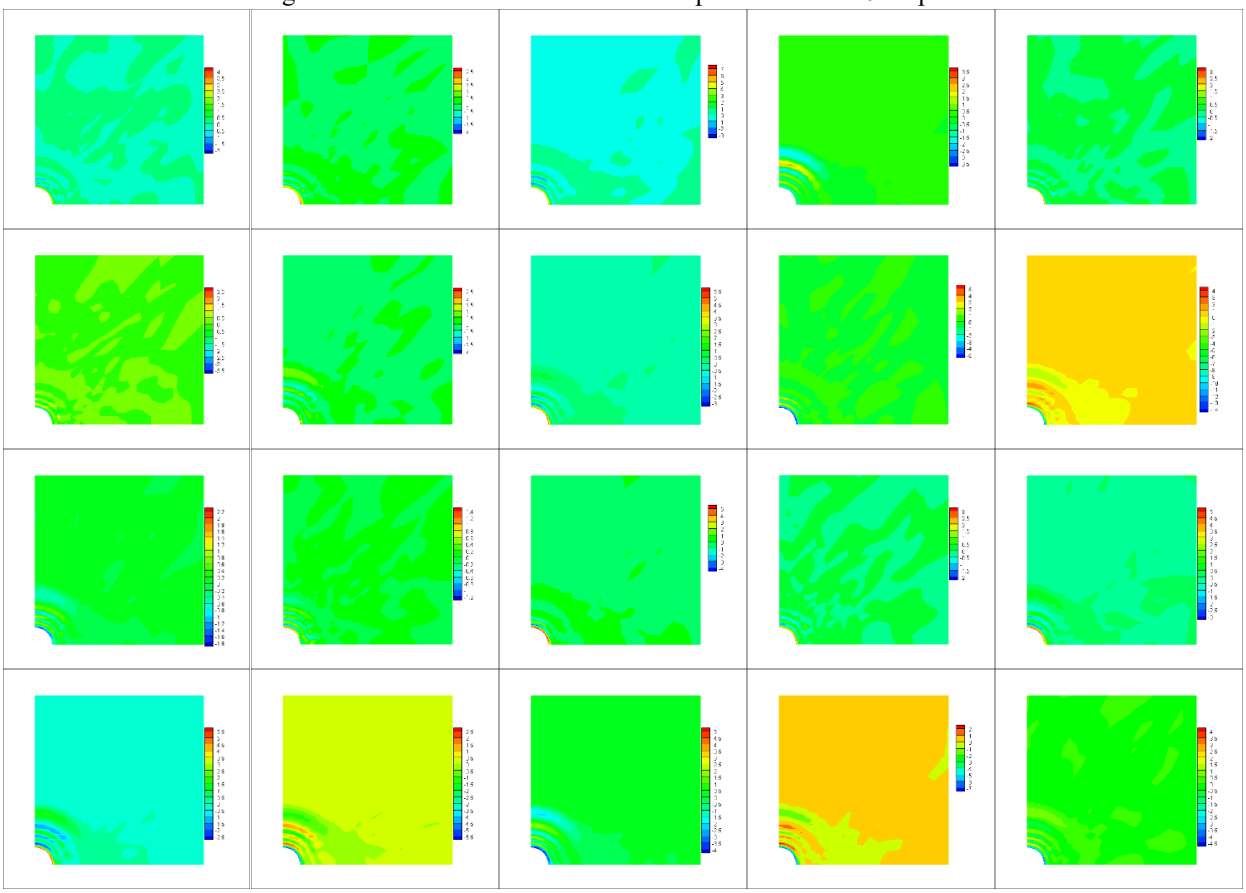

Fig. 5 The relative error of horizontal stress for 20 snapshots

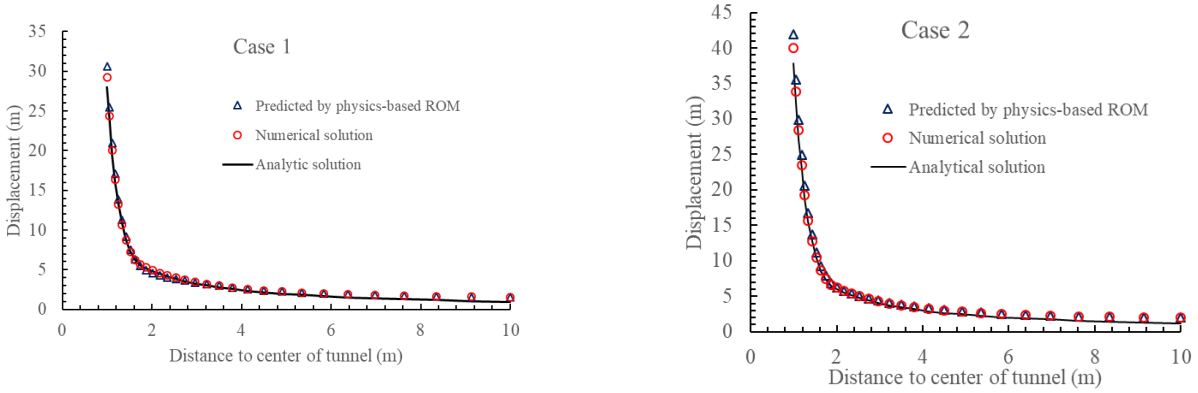

(a) Case 1 (b) Case 2

Fig. 6 Comparisons of predicted displacement of surrounding rock mass by the physics-based ROM and other techniques. (a) Case 1 (b) Case 2

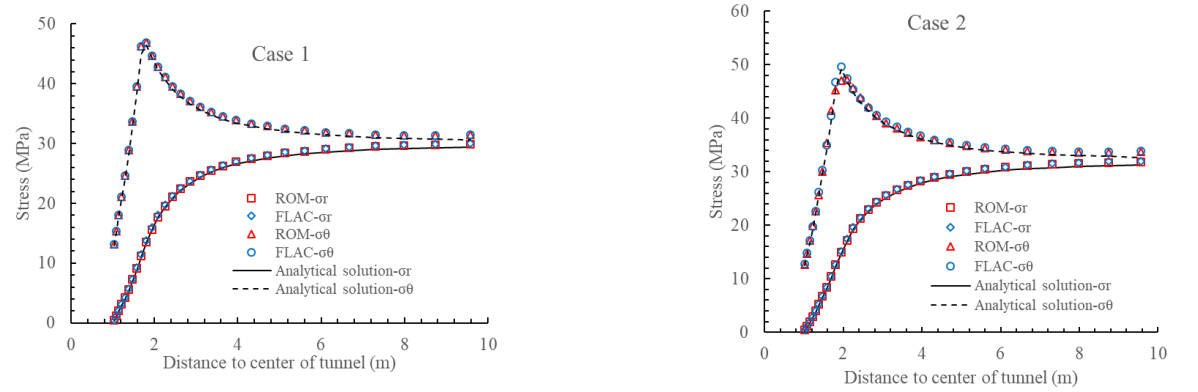

(a) Case 1 (b) Case 2

Fig. 7 Comparisons of predicted stress of surrounding rock mass by the physics-based ROM and other techniques. (a) Case 1 (b) Case 2

sets of design variables. The FLAC3D model was used to generate the snapshots for the ROM model. The snapshots of the displacement and stress field were a 3844 × 50 and 2700 × 50, respectively. The Gram matrix of design variables was a 50 × 50. Principal component analysis was used to determine the eigenfunctions based on eigenvectors of the spatial Gram matrix $\mathbf{M}^x$ and snapshots. RBF was used to compute the expanded coefficients of the ROM. The rank K of the displacement and stress field ROM are 4 and 7, respectively.

The four POD modes of the displacement field and seven POD modes of stress field are shown in Fig.3, respectively. The snapshots could be roughly approximated by the linear combinations of the first POD. The field of displacement and stress could be estimated based on the first four and seven PODs using the ROM model. The relative errors of horizontal displacement and stress are shown in Fig.4 and Fig.5, respectively. Compared with the numerical solution, the maximum relative error of horizontal displacement was about 11%, and the relative error was less than 10% for most snapshots. The maximum relative error of horizontal stress was about 7% and the relative error was less than 5% for most snapshots. These results showed that the ROM model produced solutions that were in excellent agreement with those from numerical modeling.

Thus, the ROM model can be used to approximate the displacement and stress field in the tunnel. As shown in Figs. 4 and 5, the larger relative errors occurred at the interface of the elastic and plastic zone and at the excavation boundary. The deformation and failure behaviors were complex at these locations. Furthermore, the accuracy of the ROM depended on the numerical model. In other words, the better that a numerical model represented the physical behavior of an engineering structure, the higher was the accuracy of the ROM.

Two cases were used to illustrate and verify the prediction performance of the physics-based ROM. The displacement and stress of the surrounding rock mass are shown in Figs.6 and 7. In this illustration, the numerical solutions were in excellent agreement with the analytical solution (Duncan 1993). The analytical solution presents the failure and deformation mechanism of the surrounding rock mass in the circular tunnel under the hydrostatic stress field. Figs.6 and 7 show that the ROM approximates well the displacement and stress induced by the excavated tunnel.

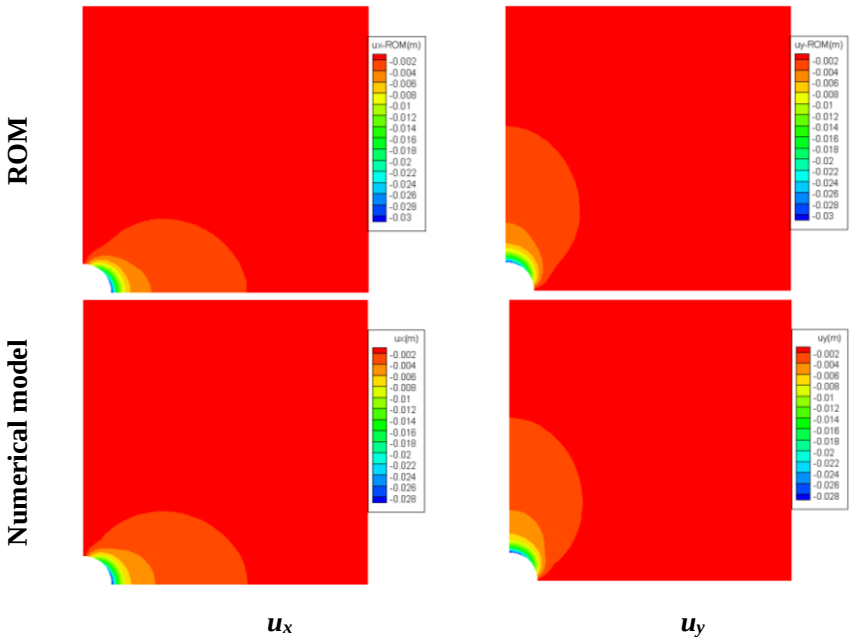

(a) Case 1

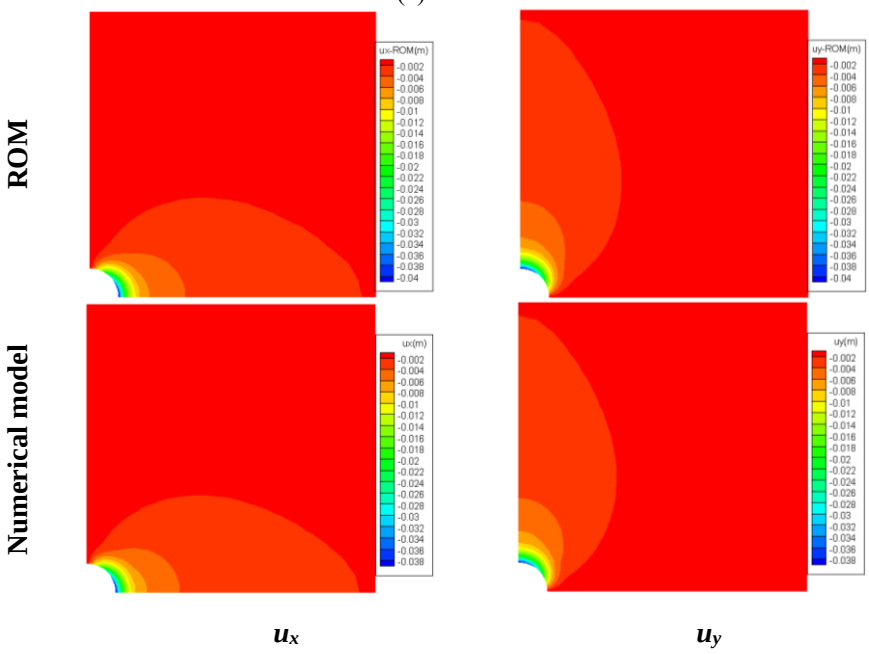

(b) Case 2

Fig. 8 Comparison of the displacement field of a circular tunnel predicted using the physics-based ROM and a numerical model. (a) Case 1 (b) Case 2.

Furthermore, the physics-based ROM model characterized well the deformation and failure mechanism of the tunnel. In addition, the error was bigger at the excavation face and interface between elastic and plastic zone. Figs.6 and 7 show that the error between the numerical solution and analytical solution was larger at these locations. These results provided additional evidence that the accuracy of the ROM depended on the numerical model. Thus, selecting a numerical model was very important to assuring the best performance of a physics-based ROM.

The predicted displacements of the surrounding rock mass by the physics-based ROM were compared with predictions from the numerical model in Fig.8. The relative error between predictions from the ROM and numerical model are shown in Fig.9. Likewise, the stress field in the surrounding rock mass predicted by the physics-based ROM was compared with that from the numerical model in Fig.10, while the errors were compared in Fig.11. The displacement and stress field predicted by the physics-based ROM were in excellent agreement with predictions of the numerical model. The maximum relative error for the displacement field predicted by the two methods was about 12% and 8% for case 1 and case 2, respectively. The maximum relative error of horizontal and vertical stress was

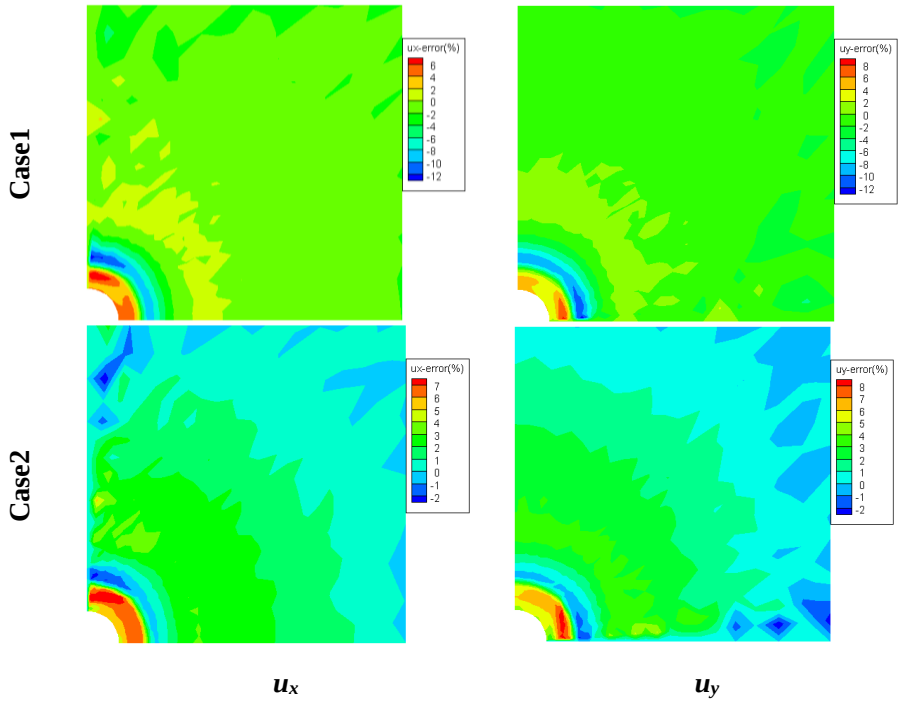

Fig. 9 The relative error between predictions of the displacement field of a circular tunnel made by the physics-based ROM and a numerical model

about 6%. However, the relative error of shear stress field predictions was greatest at the top-right corner of Fig.11. In this study, two-dimensional plane strain was adopted to simulate the excavation of the tunnel; unfortunately, this approach didn't reflect well the shear mechanism. Results presented in Figs. 8–11 again demonstrated that the accuracy of the ROM depended on the numerical model. Overall, the physics-based ROM characterized well the deformation and failure mechanism and physical laws of the geomaterials and tunnel. Thus, it could replace numerical modeling for uncertainty analysis, optimal design and back analysis, etc., all of which required repeated computations that are time-consuming and expensive.

4. Application

To further verify the physics-based ROM model, the excavation of top heading was simulated for a practical tunnel of the Nathpa Jhakri hydroelectric project in India. The span of the top heading is 10m. The properties of rock mass and engineering geological conditions associated with the project have been introduced and presented by Hoek in detail (Hoek 1999). The FLAC3D numerical model was adopted to build snapshots for the ROM model. The numerical model of the tunnel was discretized into 2450 elements and 5060 nodes (Fig.12). Hoek-Brown criterion was adopted in this study. The geological strength index (GSI), uniaxial compression strength of intact rock (σ_{ci}), the material constant (m_i), and in-situ stress were selected as the design variables. The Latin hypercube sampling (LHS) was used to generate the 200 sets of the design variables. The convergence and stress of surrounding rock mass were calculated using the numerical model and generated 200 snapshots for the ROM model. The rank K of the displacement and stress field are 7 and 58, respectively.

The above ROM model was used to estimate the convergence and stress of surrounding rock mass. The geological strength index (GSI), uniaxial compression strength of intact rock (σ_{ci}), the material constant (m_i), and in-situ stress are 45,10MPa, 10, and 6.75MPa respectively. The displacement and stress of the surrounding rock mass are shown in Figs. 13 and 14. In this application, the ROM model was in excellent agreement with the numerical solutions. Figs.13 and 14 show that the ROM model approximates well the displacement and stress induced by the excavated tunnel. It shows the physics-based ROM model can replace of numerical model to the practical tunnel.

To illustrate the ROM model, it was used to determine the extent of the convergence (the deformation of the surrounding rock mass) of the rock mass to 1000 different sets of rock mass strength and in situ stress (design variables). The result of the above were plotted in dimensionless form. Fig.15 shows the relationship between tunnel convergence and the ratio of uniaxial compressive strength of the rock mass to in situ stress. It shows the convergence of tunnel will increase dramatically when the uniaxial compressive strength of the rock mass falls below about one-tenth of the in-situ stress. It is consistent with the results of Hoek and Brown (Hoek and Brown 1997). It improved again that the physics-based ROM model characterized well the deformation mechanism of surrounding rock mass to tunnel. The running time is about 3.05 seconds to the 1000 computations using the ROM model, but the running time is about 120 seconds to one time using a numerical model. The ROM model can improve the efficiency of the computation dramatically.

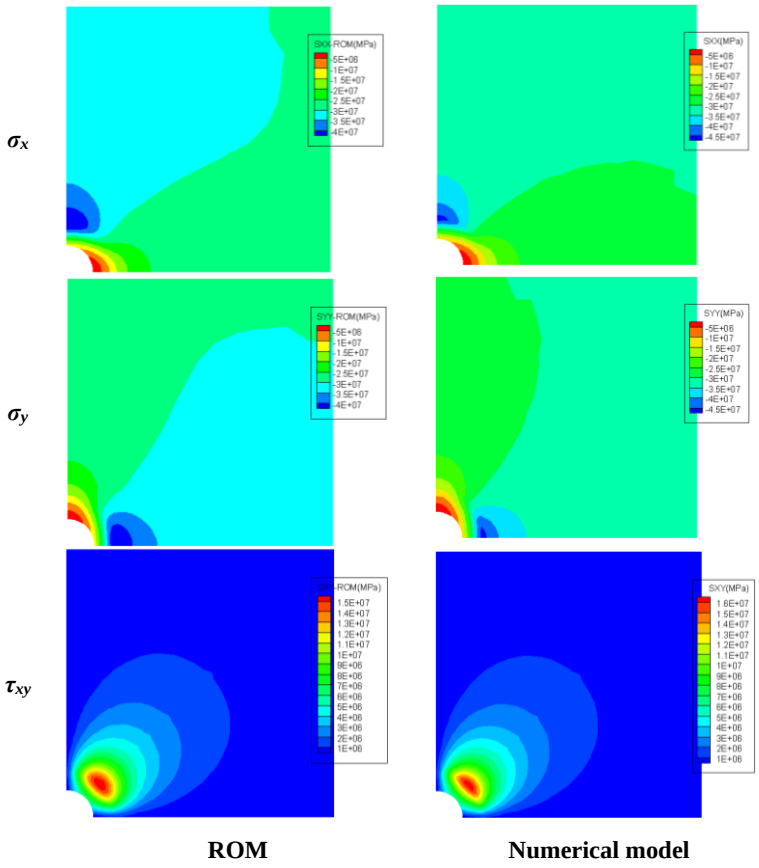

(a) Case 1

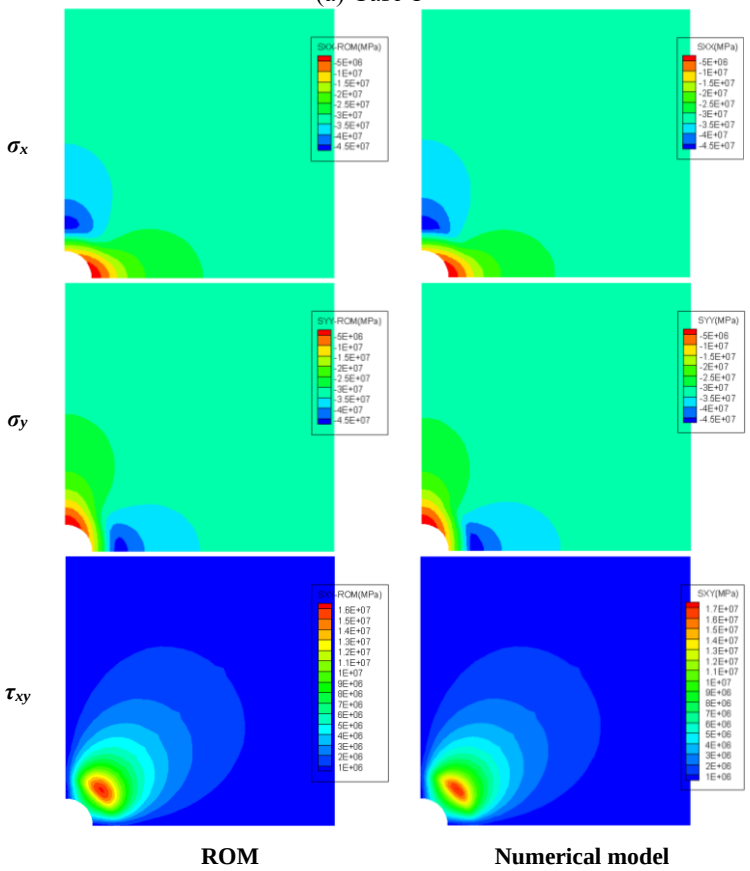

(b) Case 2

Fig. 10 Comparison of the stress field of a circular tunnel predicted using the physics-based ROM and a numerical model. (a) Case 1 (b) Case 2

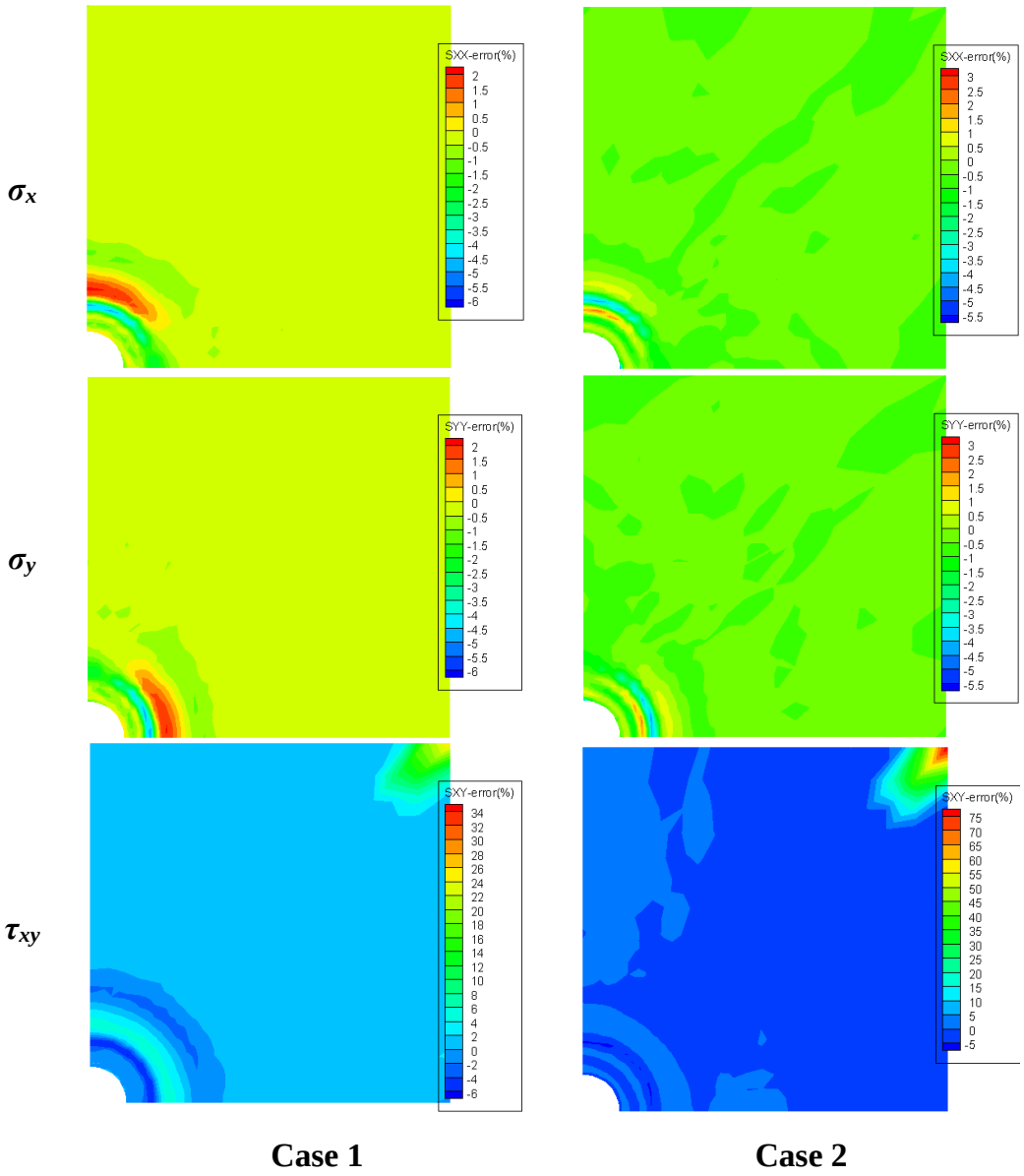

Fig. 11 The relative error between predictions of stress field of a circular tunnel made by the physics-based ROM and a numerical model

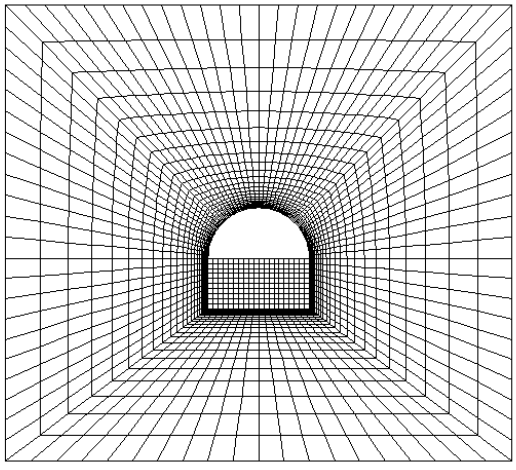

Fig. 12. The numerical model and mesh of tunnel

5. Conclusions

A physics-based ROM was developed by combining a numerical model, POD and RBF. A numerical model was used to build the snapshots using LHS. The spatial Gram matrix was constructed based on the snapshots. POD was adopted to compute the first K spatial models based on eigenvalues and eigenfunctions of the spatial Gram matrix. RBF was used to build the expanded coefficients of design variable space. The physics-based ROM was applied to a circular tunnel to illustrate and verify the application. Results showed that the physics-based ROM approximated well the displacement and stress field of the tunnel and provided an excellent characterization of the deformation and failure mechanism of the surrounding rock mass. Thus, the physics-based ROM can be used to replace numerical

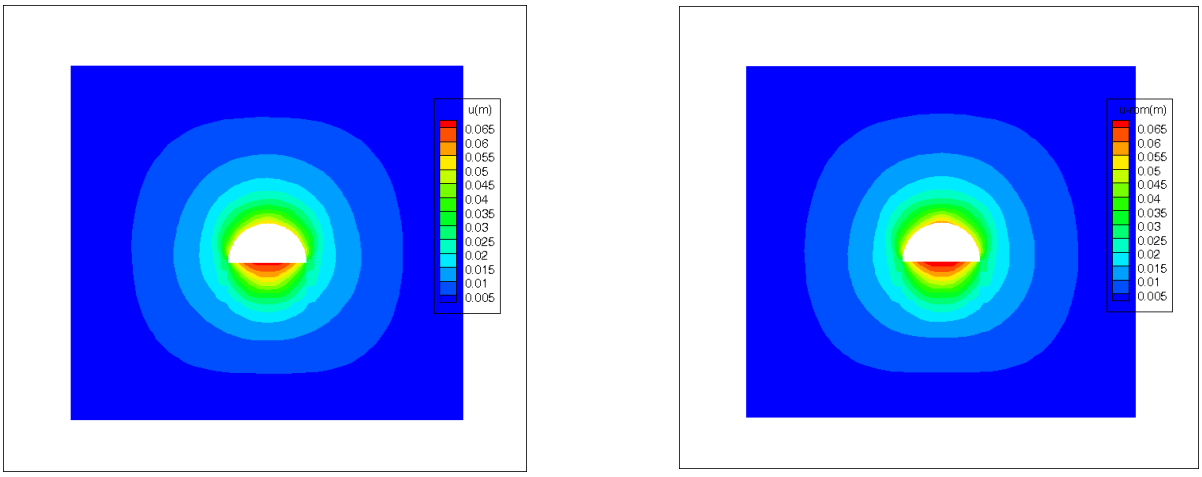

(a) Numerical model (b) ROM model

Fig. 13 The comparison between predictions of displacement field of tunnel made by the physics-based ROM and a numerical model. (a) Numerical model. (b) ROM model

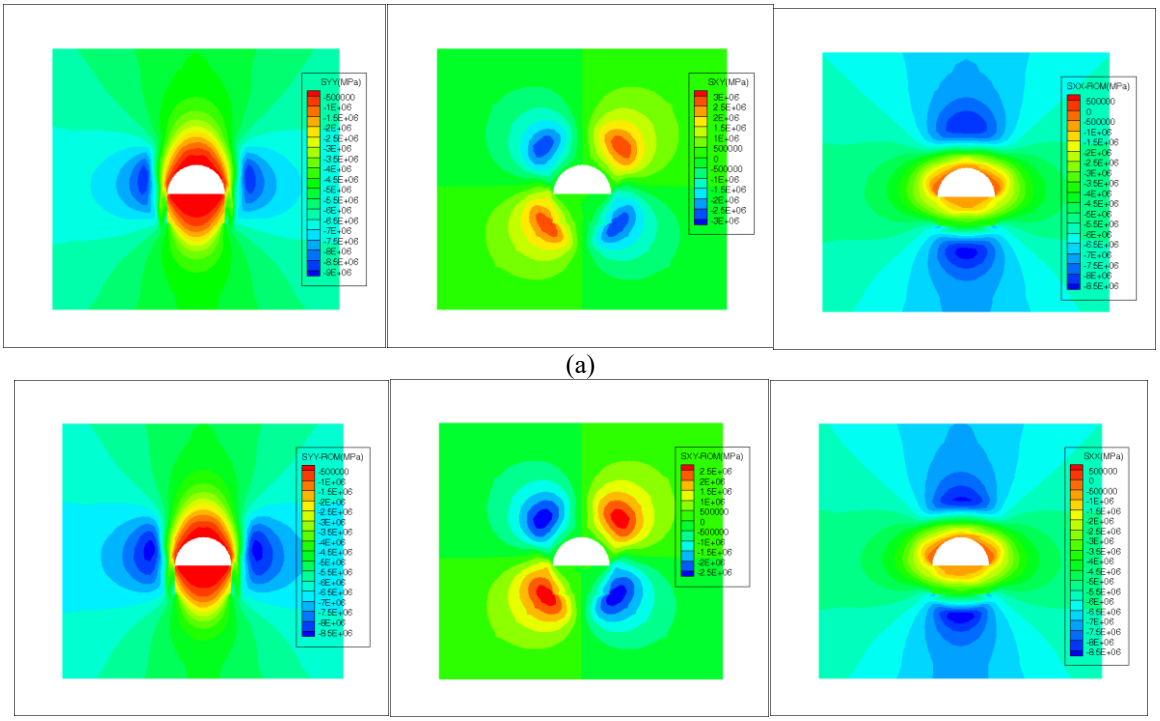

(a)

(b)

Fig. 14 The comparison between predictions of stress field of tunnel made by the physics-based ROM and a numerical model. (a) Numerical model (b) ROM model.

modeling in geotechnical engineering applications. The following specific conclusions were supported by the results of this study.

- The physics-based ROM approximated well the displacement and stress field of a tunnel. The ROM improved the efficiency of the numerical simulation and could replace a numerical model for computation of geotechnical engineering analyses. Numerical modeling was costly for practical geotechnical engineering. Specifically with regard to the repetitive computation issues such as back analysis, reliability analysis and optimal design, etc., the physics-based ROM provided an effective way to improve the efficiency of analyses and yielded highly accurate predictions.
- The physics-based ROM effectively characterized the deformation and failure mechanism associated with geotechnical engineering structures. It could represent well the physical behavior and boundary conditions.
- The parameters of RBF had a critical effect on the performance and accuracy of the physics-based ROM. Rational determination of the parameters of RBF requires further research.
- The computation time of the physics-based ROM model is significantly less than the numerical model. It improves the efficiency of the numerical model dramatically. This is important to the large-scale practical

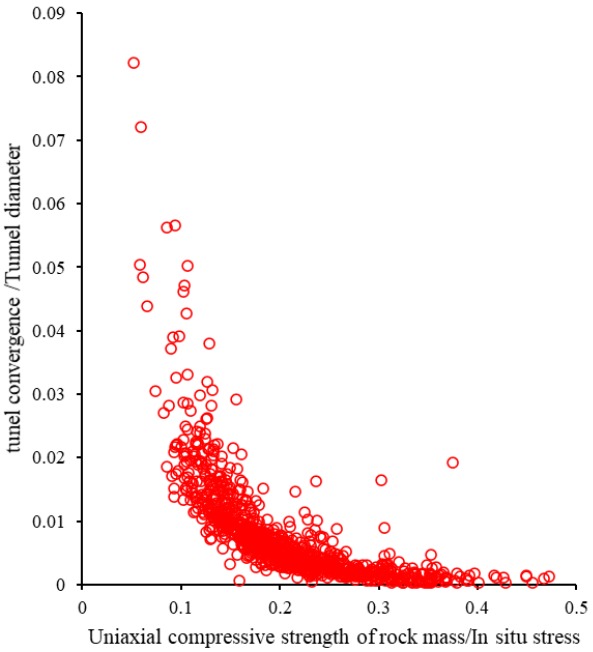

Fig. 15 Tunnel convergence versus ratio of uniaxial compressive strength of the rock mass to in situ stress

project.

- The performance and accuracy of the physics-based ROM depended on the numerical model. Selecting an appropriate numerical model was critical to the application of the physics-based ROM. To improve the performance of the physics-based ROM, the numerical model should consider and represent well the mechanical behavior and boundary conditions of the geotechnical engineering project.
- This study developed the physics-based ROM using a 2D plane strain problem with Mohr-Coulomb for rock tunnels. However, the developed model does not depend on the specific constitute model and numerical model. Further study will be implemented using other constitutive and numerical models for another geotechnical engineering in the future.

References

Aksoy, O.C., Uyar, G.G., Utku, S., Safak, S. and Ozacar, V. (2019), "A new integrated method to design of rock structures", *Geomech. Eng.*, **18**(4), 339-352. https://doi.org/10.12989/gae.2019.18.4.339.

Alipanahi, B., Delong, A., Weirauch, M.T. and Frey, B.J. (2015), "Predicting the sequence specificities of DNA- and RNA-binding proteins by deep learning", *Nature Biotech.*, **33**(8),831-838. https://doi.org/10.1038/nbt.3300.

Audouze, C., Vuyst, F.De. and Nair, P.B. (2009), "Reduced-order modeling of parameterized PDEs using time-space-parameter principal component analysis", *J. Numerical Methods Eng.*, **80** (8),1025-1057. https://doi.org/10.1002/nme.2540.

Bai, X.D., Cheng, W.C., Ong, D.E.L. and Li, G. (2021), "Evaluation of geological conditions and clogging of tunneling using machine learning", *Geomech. Eng.*, **25**(1),59-73. http://dx.doi.org/10.12989/gae.2021.25.1.059.

Bhattacharjee, S. and Matouš, K. (2020), "A nonlinear data-driven reduced order model for computational homogenization with physics/pattern-guided sampling", *Comput. Methods Appl. Mech. Eng.*, **359**, 112657. https://doi.org/10.1016/j.cma.2019.112657.

Cardoso, J.B., Almeida, J.R., Dias, J.M. and Coelho, P.G. (2008), "Structural reliability analysis using Monte Carlo simulation and neural networks", *Adv. Eng. Software*, **39**(6), 505-513. https://doi.org/10.1016/j.advengsoft.2007.03.015.

Cizmas, G.A., Richardson, B.R., Brenner, T.A., O'Brien, T.J. and Breault, R.W. (2008), "Acceleration techniques for reduced-order models based on proper orthogonal decomposition", *J. Comput. Phys*, **227**(16), 7791–7812. https://doi.org/10.1016/j.jcp.2008.04.036.

Duncan, Fama. M.E. (1993). "Numerical modeling of yield zones in weak rocks", *Comprehensive Rock Engineering Vol. 2*, Oxford, Pergamon, 49-75.

Feng, X.T., Zhao, H. and Li, S. (2004), "A new displacement back analysis to identify mechanical geo-material parameters based on hybrid intelligent methodology", *Int. J. Numer. Analytical Methods Geomech.*, **28**(11), 1141-1165. https://doi.org/10.1002/nag.381.

Fic, A., Bialecki, R.A. and Kassab, A.J. (2006), "Solving transient nonlinear heat conduction problems by proper orthogonal decomposition and the finite element method", *Numer. Heat Transfer B*, **48**(2), 102–124. https://doi.org/10.1615/ICHMT.2004.CHT-04.390.

FLAC3D 3.1 (2009), FLAC3D 3.1: Verification Problems, Itasca, Minneapolis, USA.

Freno, B.A. and Cizmas, P.G.A. (2014), "A proper orthogonal decomposition method for nonlinear flows with deforming meshes", *Int. J. Heat Fluid Flow*, **50**, 145-159. https://doi.org/10.1016/j.ijheatfluidflow.2014.07.001.

Gomes, H.M. and Awruch, A. M. (2004), "Comparison of response surface and neural network with other methods for structural reliability analysis", *Struct. Safety*, **26**(1), 49-67. https://doi.org/10.1016/S0167-4730(03)00022-5.

Haghighat, E., Raissi, M., Moure, A., Gomez, H. and Juanes, R. (2021), "A physics-informed deep learning framework for inversion and surrogate modeling in solid mechanics", *Comput. Methods Appl. Mech. Eng.*, **379**, 113741. https://doi.org/10.1016/j.cma.2021.113741.

Hamrouni, A., Dias, D and Sbartai, B. (2018), "Reliability analysis of a mechanically stabilized earth wall using the surface response methodology optimized by a genetic algorithm", *Geomech. Eng.*, **15**(4), 937-945. https://doi.org/10.12989/gae.2018.15.4.937.

Hoek, E. (1999), "Putting numbers to geology-an engineer's viewpoint", *Quarterly J. Eng. Geology Hydrogeology*, **32**(1), 1-19. https://doi.org/10.1144/GSL.QJEG.1999.032.P1.01.

Hoek, E. and Brown, E.T. (1997), "Practical estimates of rock mass strength", *Int. J. Rock Mech. Mining Sci.*, **34**(8), 1165-1186. https://doi.org/10.1016/S0148-9062(97)00305-7.

Huys, Quentin. J.M., Maia, Tiago. V. and Frank, Michael. J. (2016), "Computational psychiatry as a bridge from neuroscience to clinical applications", *Nature Neurosci.*, **19**(3), 404-413. https://doi.org/10.1038/nn.4238.

Jain, P. and Chakraborty, T. (2018), "Numerical analysis of tunnel in rock with basalt fiber reinforced concrete lining subjected to internal blast load", *Comput. Concrete*, **21**(4), 399-406. https://doi.org/10.12989/cac.2018.21.4.399.

Jing, L. and Hudson, J.A. (2002), "Numerical methods in rock mechanics", *Int. J. Rock Mech. Mining Sci.,* **39**(4),409-427. https://doi.org/10.1016/S1365-1609(02)00065-5.

Kathirvel, P. and Kaliyaperumal, S.R.M. (2017), "Probabilistic modeling of geopolymer concrete using response surface

methodology", *Comput. Concrete*, **19**(6), 737-744. https://doi.org/10.12989/cac.2017.19.6.737.

Kenneth, C., Hall, Jeffrey. P. Thomas., and Earl, H. Dowell. (2000), "Proper orthogonal decomposition technique for transonic unsteady aerodynamic flows", *AIAA J.*, **38**(10),1853-1862. https://doi.org/10.2514/2.867.

LeCun, Y., Bengio, Y. and Hinton, G. (2015), "Deep learning", *Nature*, **521**, 436-444. https://doi.org/10.1038/nature14539.

Li, D.Q., Zheng, D., Cao, Z.J., Tang, X.S. and Phoon, K.K. (2016), "Response surface methods for slope reliability analysis: Review and comparison", *Eng. Geology*, **203**(25), 3-14. https://doi.org/10.1016/j.enggeo.2015.09.003.

Li, Z., Liu, J., Xu, R., Liu, H. and Shi, W. (2021), "Study of grouting effectiveness based on shear strength evaluation with experimental and numerical approaches", *Acta Geotechnica*, https://doi.org/10.1007/s11440-021-01324-4.

Liu, J., Jiang,Y., Zhang, Y. and Sakaguchi, O. (2021), "Influence of different combinations of measurement while drilling parameters by artificial neural network on estimation of tunnel support patterns", *Geomech. Eng.*, **25**(6), 439-454. http://dx.doi.org/10.12989/gae.2021.25.6.439.

Lopes, P.A.M., Gomes H.M. and Awruch, A.M. (2010), "Reliability analysis of laminated composite structures using finite elements and neural networks", *Compos. Structures*, **92**(7), 1603-1613. https://doi.org/10.1016/j.compstruct.2009.11.023.

Luat, N.V., Lee, K. and Thai, D.K. (2020), "Application of artificial neural networks in settlement prediction of shallow foundations on sandy soils", *Geomech. Eng.*, **20**(5), 385-397. http://dx.doi.org/10.12989/gae.2020.20.5.385.

Luo, Z., Gao, J. and Xie, Z. (2015), "Reduced-order finite difference extrapolation model based on proper orthogonal decomposition for two-dimensional shallow water equations including sediment concentration", *J. Math. Anal. Appl.*, **429**(2), 901–923. https://doi.org/10.1016/j.apm.2012.10.051.

Lv, Q. and Low, B.K. (2011), "Probabilistic analysis of underground rock excavations using response surface method and SORM", *Comput. Geotech.*, **38**(8),1008-1021. https://doi.org/10.1016/j.compgeo.2011.07.003.

Mahdevari, S. and Torabi, S.R. (2012), "Prediction of tunnel convergence using Artificial Neural Networks", *Tunnel Underground Space Technol.*, **28**(1), 218-228. https://doi.org/10.1016/j.tust.2011.11.002.

Mahdevari, S., Torabi, S.R. and Monjezi, M. (2012), "Application of artificial intelligence algorithms in predicting tunnel convergence to avoid TBM jamming phenomenon", *Int. J. Rock Mech. Min. Sci*, **55**, 33-44. https://doi.org/10.1016/j.ijrmms.2012.06.005.

Mathew, T.V., Prajith, P., Ruiz, R.O., Atroshchenko, E. and Natarajan, S. (2020), "Adaptive importance sampling based neural network framework for reliability and sensitivity prediction for variable stiffness composite laminates with hybrid uncertainties", *Compos. Struct.*, **245**, 112344. https://doi.org/10.1016/j.compstruct.2020.112344.

Myers, R.H., Montgomery, D.C. and Anderson-Cook, C.M. (2009), *Response Surface Methodology-Process and Product Optimization Using Designed Experiments 3rd edition*, Wiley, New Jersey, USA.

Oh, J., Moon, T., Canbulat, I. and Moon, J.S. (2019), "Design of initial support required for excavation of underground cavern and shaft from numerical analysis", *Geomech. Eng.*, **17**(6), 573-581. https://doi.org/10.12989/gae.2019.17.6.573.

Pichler, B., Lackner, R. and Mang, H.A. (2003), "Back analysis of model parameters in geotechnical engineering by means of soft computing", *J. Numer. Meth. Eng.*, **57**(14), 1943-1978. https://doi.org/10.1002/nme.740.

Rafiai, H. and Moosavi, M. (2012), "An approximate ANN-based solution for convergence of lined circular tunnels in elasto-plastic rock masses with anisotropic stresses", *Tunnel Underground Space Technol.*, **27**(1), 52-59. https://doi.org/10.1016/j.tust.2011.06.008.

Reichstein, M., Camps-Valls, G., Stevens, B., Jung, M., Denzler, J. and Carvalhais, N. (2019), "Deep learning and process understanding for data-driven earth system science", *Nature*, **566**,195-203. https://doi.org/10.1038/s41586-019-0912-1.

Saseendran, R. and Dodagoudar G.R. (2020), "Reliability analysis of slopes stabilised with piles using response surface method", *Geomech. Eng.*, **21**(6), 513-525. https://doi.org/10.12989/gae.2020.21.6.513.

Severson, K. A., Attia, P. M., Jin, N., Perkins, N., Jiang, B., Yang, Z., Chen, M.H., Aykol, M., Herring, P.K., Fraggedakis, D., Bazant, M.Z., Harris, S.J., Chueh, W.C. and Braatz, R. D. (2019), "Data-driven prediction of battery cycle life before capacity degradation", *Nature Energy*, **4**, 383-391. https://doi.org/10.1038/s41560-019-0356-8.

Tang, M., Liu, Y. and Durlofsky, L.J. (2020), "A deep-learning-based surrogate model for data assimilation in dynamic subsurface flow problems", *J. Comput. Physics*, **413**, 109456. https://doi.org/10.1016/j.jcp.2020.109456.

Thakur, S.N., Chakraborty, S. and Ray, C. (2019), "Reliability analysis of laminated composite shells by response surface method based on HSDT", *Struct. Eng. Mech.*, **72**(2), https://doi.org/10.12989/sem.2019.72.2.203.

Veer, L.J. and Bernards, R. (2008), "Enabling personalized cancer medicine through analysis of gene-expression patterns", *Nature*, **452**, 564-570. https://doi.org/10.1038/nature06915.

You, K. (2014), "A case study on the utilization of tunnel face mapping data for a back analysis based on artificial neural network", *KSCE J. Civil Eng.*, **18**, 751-759. https://doi.org/10.1007/s12205-014-0329-1.

Zhang, B., Ma, Z., Wang, X., Zhang, J. and Peng, W. (2020), "Reliability analysis of anti-seismic stability of 3D pressurized tunnel faces by response surfaces method", *Geomech. Eng.*, **20**(1), 43-54. https://doi.org/10.12989/gae.2020.20.1.043.

Zhao, H. (2008), "Slope reliability analysis using a support vector machine", *Comput. Geotech.*, **35**(3), 459–467. https://doi.org/10.1016/j.compgeo.2007.08.002.

Zhao, H. (2021), "A reduced order model based on machine learning for numerical analysis: An application to geomechanics", *Eng. Appl. Artificial Intelligent*, **100**, 104194. https://doi.org/10.1016/j.engappai.2021.104194.

Zhao, H. and Yin, S. (2016), "Inverse analysis of geomechanical parameters by artificial bee colony algorithm and multi-output support vector machine", *Inverse Problems Sci. Eng.*, **24**(7), 1266-1281. https://doi.org/10.1080/17415977.2016.1178257.

Zhao, H., Chen, B. and Li, S. (2021), "Determination of geomaterial mechanical parameters based on back analysis and reduced-order model", *Comput. Geotech.*, **132**, 104013. https://doi.org/10.1016/j.compgeo.2021.104013.

Zhao, H., Chen, B., Li, S., Li, Z. and Zhu, C. (2021), "Updating models and the uncertainty of mechanical parameters for rock tunnels using Bayesian inference", *Geosci. Frontiers*, **12**(5), 101198. https://doi.org/10.1016/j.gsf.2021.101198.

Zhao, H.B. and Yin, S.D. (2009), "Geomechanical parameters identification by particle swarm optimization and support vector machine", *Appl. Math Model*, **33**(10), 3997-4012. https://doi.org/10.1016/j.apm.2009.01.011.

Zienkiewicz, O.Z., Taylor, R.L. and Zhu, J.Z. (2005), *The Finite Element Method: Its Basis and Fundamentals*, Sixth edition, Elsevier, Singapore, Singapore.

GC